Available online at www.sciencedirect.com

ScienceDirect

Procedia CIRP 00 (2023) 000–000

www.elsevier.com/locate/procedia

17th CIRP Conference on Intelligent Computation in Manufacturing Engineering

Cutting force estimation from machine learning and physics-inspired data-driven models utilizing accelerometer measurements

Gregory W. Vogl[a,*], Yongzhi Qu[b], Reese Eischens[b], Gregory Corson[c], Tony Schmitz[c,d], Andrew Honeycutt[d], Jaydeep Karandikar[d], and Scott Smith[d]

[a]*Engineering Laboratory, National Institute of Standards and Technology (NIST), 100 Bureau Drive, Gaithersburg, Maryland 20899-8220, USA*
(Official contribution of the National Institute of Standards and Technology; not subject to copyright in the United States.)
[b]*Mechanical & Industrial Engineering Department, University of Minnesota Duluth, Duluth, MN 55812, USA*
[c]*Department of Mechanical, Aerospace, and Biomedical Engineering, University of Tennessee, Knoxville, Tennessee 37996, USA*
[d]*Manufacturing Demonstration Facility, Oak Ridge National Laboratory, Knoxville, Tennessee 37932, USA*

* Corresponding author. Tel.: +01-301-975-3198 ; Fax: +01-301-975-8058. *E-mail address:* gvogl@nist.gov

Abstract

Monitoring cutting forces for process control may be challenging because force measurements typically require invasive instrumentation. To remedy this situation, two new methods were recently developed to estimate cutting forces in real time based on the use of on-machine accelerometer measurements. One method uses machine learning, while another uses a physics-inspired data-driven approach, to generate a model that estimates cutting forces from on-machine accelerations. The estimated forces from both approaches were compared against cutting force data collected during various milling operations on several machine tools. The results reveal the advantages and disadvantages of each model to estimate real-time cutting forces.

Peer-review under responsibility of the scientific committee of the 17th CIRP Conference on Intelligent Computation in Manufacturing Engineering, 12-14 July, Gulf of Naples, Italy

Keywords: Smart manufacturing; Industry 4.0; Data-driven dynamics; Frequency response function; Machine tool; Modeling; Dynamics; Machining processes; Sensing; Monitoring; Diagnostics

1. Introduction

Machine tools have progressed from being manually driven to being extremely automated, yet real-time knowledge of performance and mechanical degradation may still be in its infancy. Hence, the future of smart manufacturing, or Industry 4.0, will rely upon dependable, robust, and relatively inexpensive monitoring systems [1, 2] to track the health of machines and their processes. Systems with integrated sensors and associated analytics for monitoring the errors and mechanical conditions of linear axes and spindles as well as the machine's thermal displacements would help to enable the future vision of Industry 4.0.

One potentially significant enabler would be spindles with integrated accelerometers [3, 4] or other inexpensive sensors to estimate cutting forces and track tool wear and other performance metrics in real time. Such an intelligent spindle system would be a true enabler of smart manufacturing because, although lower cost options have been proposed [5-9], measuring cutting forces currently requires invasive and relatively expensive sensors, such as dynamometers. In contrast, accelerometers can be fixtured within machine tool spindle housings and can have relatively high bandwidths and sensitivities, which may prove useful to track high frequency cutting forces.

Peer-review under responsibility of the scientific committee of the 17th CIRP Conference on Intelligent Computation in Manufacturing Engineering, 12-14 July, Gulf of Naples, Italy

However, creating a method to estimate the cutting forces from accelerations for any spindle speed, force profile, tool type, and cutting conditions is challenging. Such a task requires knowledge of how forces relate to accelerations, which first requires on-machine measurements. Accordingly, a spindle metrology suite was developed to measure magnetic forces induced by a rotating magnet on an instrumented tool holder while accelerometers measure on-machine vibrations [10]. This process simulates cutting because of the cyclic forces from the interaction of rotating and stationary magnets. A dataset of synchronized accelerations and forces is collected for various combinations of spindle speeds and forces. Then, the "simulated cutting dataset" may be used to create models that input the accelerations and output the forces for any spindle speed and force level.

This paper compares two approaches to estimate cutting forces based on the use of on-machine accelerations. One method uses machine learning, while another uses a physics-inspired data-driven approach [10]. The modeled forces from both approaches were compared against cutting force data measured during milling operations on two machine tools.

2. Experimental setup

Fig. 1 shows the first experimental setup on a vertical machining center (VMC). Two triaxial integrated electronic piezoelectric (IEPE) ground-isolated accelerometers (PCB Piezotronics J356A45) with nominal sensitivities of 10.2 mV/(m/s²) (100 mV/g) were epoxied with high-temperature epoxy (Permatex 84102) to the spindle face of the VMC (Haas VF-4). The instrumented tool holder containing a NeFeB magnet was placed in the spindle. During rotation, the rotating magnet of the tool holder interacts with stationary magnets on commercial strain-gauge-based force-torque sensors (ATI Industrial Automation Mini45) in the metrology suite, causing magnetic forces that simulate cutting. The resulting forces and vibrations are measured by the data acquisition (DAQ) box.

To create the simulated cutting dataset used to generate models that relate forces and accelerations, data was collected for various spindle speeds and force levels. To set the force levels, each stationary magnet of the metrology suite was moved via its linear positioning stage, and the Z-axis position of the instrumented tool holder was moved vertically, to produce the desired ranges of the magnetic forces in the X-, Y-, and Z-axis directions during rotation of the instrumented tool holder. Then, for that given configuration, the DAQ box collects the force and acceleration data repeatedly at 51.2 kHz over a duration of 1 s while the spindle speed increases from 500 rpm to 7500 rpm in a stepwise manner with an increment of 100 rpm over a period of about 7 min. Next, a new configuration of the magnets was chosen to produce different magnetic forces, and data were collected during the same stepwise increase of the spindle speed from 500 rpm to 7500 rpm. The highest force range was about 80 N, while the lowest force range was about 1 N. The variety of combinations of directional forces, and hence the variety of combinations of X-, Y-, and Z-axis accelerations, should aid in distinguishing the relationships of accelerations to forces for the models. In total, simulated cutting data were collected for 639 combinations of spindle speeds and force configurations. Table 1 shows the relative qualitative force ranges for the nine utilized magnet configurations.

Table 1. Relative qualitative force ranges for each configuration of magnets.

	Relative Qualitative Force Range		
Configuration Number	X-axis	Y-axis	Z-axis
1	Low	Low	Low
2	Medium	Low	Low
3	High	Low	Low
4	Low	Medium	Low
5	Low	High	Low
6	Medium	Low	Medium
7	High	Low	Medium
8	Low	Medium	Medium
9	Low	High	Medium

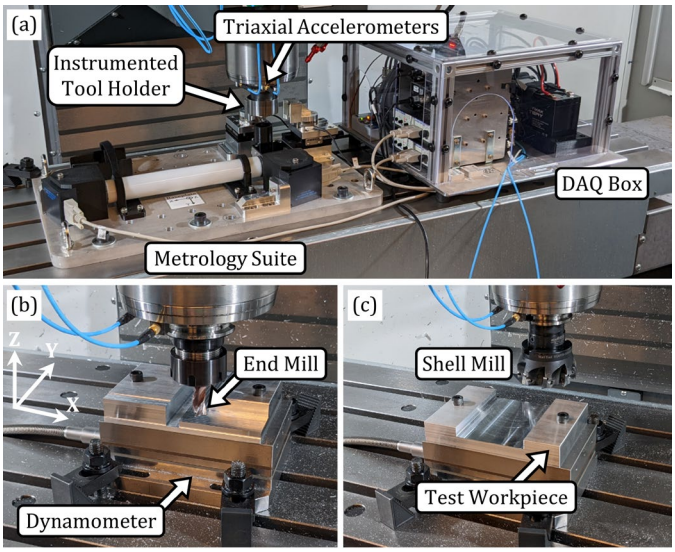

Fig. 1. (a) Metrology suite and instrumented tool holder on vertical machining center, (b) end mill with dynamometer, and (c) shell mill with dynamometer.

After collection of the simulated cutting dataset, the instrumented tool holder, DAQ box, and metrology suite were removed from the machine tool and the dynamometer was attached to the worktable within the machine tool, as seen in Fig. 1b. An Al 6061-T6 workpiece was then installed on top of the dynamometer. Consequently, the dynamometer and on-machine accelerometers were the only sensors remaining in the machine tool for data collection during cutting of the workpiece. As seen in Fig. 1b, a three-fluted end mill with a diameter of 12.70 mm (0.5 in) and an overhang length of 36.72 mm (1.4455 in) was inserted into a CAT-40 collet chuck and used to down mill the workpiece in the X-axis and Y-axis directions. Then, as seen in Fig. 1c, a new workpiece was installed on the dynamometer and an eight-toothed indexable shell mill with a diameter of 76.2 mm (3 in) and an overhang length of 79.38 mm (3.125 in) was used to down mill the workpiece in the Y-axis direction. Forces were

sampled by the dynamometer at 50 kHz and accelerations were sampled at 51.2 kHz, both with various record lengths, to capture cutting forces and machine accelerations before, during, and after each cutting pass.

Fig. 2 shows the second experimental setup on a horizontal machining center (HMC). As seen in Fig. 2a, the simulated cutting dataset was collected for the HMC (Makino a51nx) in the same manner as for the VMC. Then, the cutting passes were performed. A three-fluted end mill with a diameter of 12.70 mm (0.5 in) and an overhang length of 74.96 mm (2.951 in) in a heat shrink holder was used to down mill the workpiece in the X-axis direction (see Fig. 2b). Forces were sampled by the dynamometer at 50 kHz and accelerations were sampled at 51.2 kHz before, during, and after each pass.

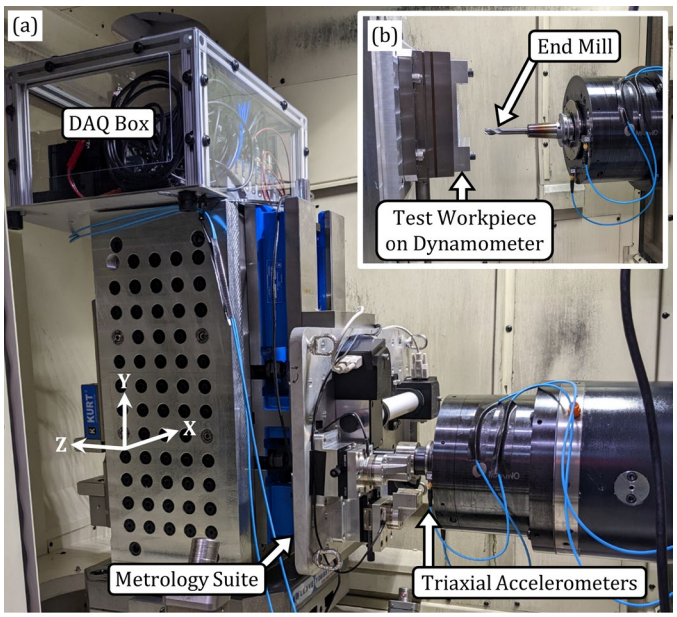

Fig. 2. (a) Simulated cutting setup within horizontal machining center and (b) cutting setup with end mill, dynamometer, and accelerometers.

3. Models for force estimation from accelerations

Two models, based on separate approaches, were created for each of the machine tool datasets described in Sec. 2 to estimate cutting forces using accelerations from only one triaxial accelerometer. The models are described in this section and then compared in the following sections to understand their advantages and disadvantages.

The first approach is a machine learning (ML) method that uses deep neural networks for regression. A data-driven regression method with a learned nonlinear basis has been proposed to learn the frequency response function (FRF) and was previously shown to estimate simulated cutting (i.e., magnetic) forces with a relatively high accuracy [11]. That method was tested for the simulated cutting datasets described in Sec. 2, but due to the limited amount of training data, the models could not converge. Instead, a simpler deep neural network (DNN) model was constructed for FRF learning. The DNN model contains [7, 30, 50, 50, 10, 1] nodes in each of its six layers, respectively. The DNN model inputs the real and imaginary parts of each triaxial vibration spectrum component as well as its frequency and outputs the force spectrum component at the corresponding frequency. The DNN model uses the Fast Fourier transform (FFT) data to predict the actual cutting forces, for the first time, up to 500 Hz.

The second approach is a physics-inspired (PI) data-driven model [10] that accounts for pre-defined (not learned) nonlinearity types. Specifically, the model accounts for up to quadratic dependencies on spindle speed but does not account for other nonlinearities. Unlike the first model, the second model is from a non-ML approach. The PI model results in speed-dependent FRFs approximated by solving for discrete FRF values from a least-squares fit. Previously, the original method [10] used FFT data with signal-to-noise ratios (SNR) greater than 20 to solve for FRF values every 5 Hz.

However, the PI method was modified such that each signal is fitted with harmonics up to 500 Hz and those coefficients are used to create each model by solving for FRF values at frequencies with varied spacings between 5 Hz and 18 Hz. Elimination of a SNR constraint was needed because the accelerometers were changed to have a 10X higher range to allow for greater acceleration magnitudes but resulted in higher noise and lower SNRs. Using Fourier components partially mitigates the lower SNRs and also produces estimated forces that are strictly periodic. Furthermore, the adaptive frequency spacing between 5 Hz and 18 Hz was used to nominally produce at least 150 data points within each frequency bin, which helps to avoid both overfitting (small spacings; too few data per model variable) and underfitting (large spacings; too much data per model variable).

Finally, other changes were implemented to create the PI model that handles low SNRs. First, 1000 models were created with random samplings of half of the simulated cutting data. These models have different FRFs due to their different data combinations used for the least-squares solution. Then, the five percent of the models (50 models) having the lowest root mean square error (RMSE) metric values (see Sec. 4) were averaged to create a final model.

All data-driven models, whether ML or PI, output estimated forces with frequencies up to 500 Hz but not down to 0 Hz. IEPE accelerometers do not have bandwidths down to 0 Hz, so estimation of steady-state forces is not possible with this setup. Accordingly, all signals have their steady-state components removed and only the alternating current (AC) components were used for the following results.

4. Metrics for comparison

Both ML and PI models output forces, so the performances of the models can be compared via the use of various metrics. The metrics depend upon the force deviation, δ_{ij}, which is the difference between the modeled and measured forces; that is,

$$\delta_{ij} = \hat{F}_{ij} - F_{ij} \tag{1}$$

where $\hat{F}_{ij}$ is the j^{th} data point in the i^{th} modeled force signal, and F_{ij} is the j^{th} data point in the i^{th} measured force signal.

Three metrics for the i^{th} comparison are the mean absolute error (MAE_i), the root mean square error (RMSE_i), and the maximum absolute error (MaxAE_i), defined as

$$\text{MAE}_i = \frac{1}{m_i}\sum_{j=1}^{m_i}\left|\delta_{ij}\right| \tag{2}$$

$$\mathrm{RMSE}_i = \sqrt{\frac{1}{m_i}\sum_{j=1}^{m_i}\delta_{ij}^2} \quad (3)$$

$$\mathrm{MaxAE}_i = \max\left(\left|\delta_{ij}\right| \forall\, j\right) \quad (4)$$

where m_i is the number of data points in each i^{th} force signal. Equations (2)-(4) yield three populations (or vectors) of metric values, each having a length of n, which is the number of force signals within the given dataset. If the metric values are for a simulated cutting dataset, then $n = 639$ because there are 639 data files, one for each force signal based on a unique combination of spindle speed and force configuration. Naturally, these error metric populations may be statistically analyzed, e.g., via means and standard deviations. Also, the mean range (M-R) for all measured force signals is a useful measure and is defined as

$$\text{M-R} = \frac{1}{n}\sum_{i=1}^{n}\left[\max\left(F_{ij} \forall\, j\right) - \min\left(F_{ij} \forall\, j\right)\right] \quad (5)$$

Therefore, for a given machine tool, each model yields three populations of overall error metrics (MAE, RMSE, MaxAE) for the simulated cutting dataset, as measures of the model's training performance, as well as a different set of overall error metric populations for the actual cutting dataset, as measures of the model's prediction performance.

5. Comparison of model training performances

Table 2 and Table 3 show the training performance metrics of the models for the VMC and the HMC, respectively, based on use of the associated simulated cutting (magnetic force) datasets. Each simulated cutting dataset is composed of 639 data files with synchronized accelerations and magnetic forces that were each collected over a duration of 1 s. The accelerations were inserted into each model to output the X-, Y-, and Z-axis force estimates for comparison with the measured forces. The overall error metrics are reported in the form of "mean ± standard deviation," based on the error metric populations defined in Eqs. (2)-(4). The mean force range (M-R) of the measured data is also shown in the tables for comparison purposes.

Table 2. Training performance metrics for the ML and PI models for the VMC with its associated simulated cutting dataset.

		Metric			
Force	Model	MAE (N)	RMSE (N)	MaxAE (N)	M-R (N)
F_X	ML	3.248 ± 2.411	4.027 ± 3.039	10.584 ± 8.435	24.72
	PI	2.821 ± 1.346	3.438 ± 1.652	7.395 ± 3.831	
F_Y	ML	3.252 ± 2.417	4.026 ± 3.020	10.435 ± 8.007	23.62
	PI	3.017 ± 1.570	3.633 ± 1.891	7.550 ± 4.110	
F_Z	ML	0.764 ± 0.515	0.961 ± 0.676	2.521 ± 1.959	4.653
	PI	1.039 ± 0.370	1.322 ± 0.482	3.175 ± 1.332	

As seen in Table 2 and Table 3, the PI and ML models estimate the magnetic forces with average MAEs of roughly 15 percent of the mean force ranges (M-Rs). However, the PI models are slightly more accurate, in general, than the ML models because the PI models produce metric populations with standard deviations that are relatively smaller compared to the corresponding means.

Table 3. Training performance metrics for the ML and PI models for the HMC with its associated simulated cutting dataset.

		Metric			
Force	Model	MAE (N)	RMSE (N)	MaxAE (N)	M-R (N)
F_X	ML	3.952 ± 2.649	4.877 ± 3.297	12.616 ± 8.634	29.27
	PI	3.153 ± 1.668	3.796 ± 2.007	7.744 ± 4.234	
F_Y	ML	3.583 ± 2.220	4.444 ± 2.789	11.882 ± 7.264	25.75
	PI	2.474 ± 1.172	2.945 ± 1.363	5.959 ± 2.612	
F_Z	ML	1.225 ± 0.679	1.530 ± 0.864	3.960 ± 2.397	7.183
	PI	1.204 ± 0.456	1.537 ± 0.582	3.704 ± 1.515	

6. Comparison of model prediction performances

It is worth noting again that the model training is only performed with the simulated cutting data while the real cutting data is reserved for prediction purposes, because every model must demonstrate its interpolation and extrapolation capabilities on unforeseen data. Accordingly, Table 4 and Table 5 show the testing performance metrics of the models for the VMC and the HMC, respectively, based on use of the associated cutting datasets. Accelerometer and dynamometer data were recorded for 37 cutting passes for the VMC and 18 cutting passes for the HMC. For each cutting pass, the accelerometer data during 1 s of the dynamic steady state in the middle of the pass were inputted into the models to output the X-, Y-, and Z-axis force estimates. Because the accelerometer data was not synchronized to the dynamometer data in the middle of the cut, being collected by different systems without triggering, each measured force was aligned (shifted in time) to its associated modeled force to minimize the RMSE (see Eq. (3)) between the two signals. After this alignment was performed for each pair of modeled and measured forces, the overall error metric populations defined in Eqs. (2)-(4) were utilized in Table 4 and Table 5 in the form of "mean ± standard deviation." The mean force range (M-R) of the measured data is also shown in the tables for comparison purposes.

As seen in Table 4 and Table 5, the PI models estimate the cutting forces with average MAEs of roughly 20 percent of the mean force ranges (M-R values). This relative error is slightly greater than its value of around 15 percent for the simulated cutting datasets (see Table 2 and Table 3). Therefore, the PI models perform almost as well for the actual cutting datasets as for the simulated cutting datasets used for training. This consistent performance is fairly impressive when considering that (1) the cutting forces are generally more than 10X greater in magnitude than the magnetic forces on which the models were trained and (2) the cutting components may be dominated by harmonics due to multiple cutting teeth, which is not the case for the magnetic force components. In contrast, the ML models estimate the cutting

forces with average MAEs of roughly 30 percent of the mean force ranges, which is a significant decrease in performance compared to its training performance. Also, the standard deviations of the MAE testing populations for the ML models are about twice as large as those for the PI models.

Table 4. Testing performance metrics for the ML and PI models for the VMC with its associated cutting dataset.

		Metric			
Force	Model	MAE (N)	RMSE (N)	MaxAE (N)	M-R (N)
F_X	ML	52.46 ± 35.04	61.84 ± 40.23	132.98 ± 83.33	259.9
	PI	38.41 ± 17.09	46.43 ± 20.45	102.99 ± 49.67	
F_Y	ML	67.04 ± 58.39	80.32 ± 72.27	164.58 ± 133.03	275.1
	PI	55.63 ± 35.12	66.31 ± 41.51	136.68 ± 86.45	
F_Z	ML	18.93 ± 15.74	22.51 ± 20.07	46.88 ± 34.95	78.06
	PI	10.76 ± 3.60	13.36 ± 4.60	31.92 ± 13.18	

Table 5. Testing performance metrics for the ML and PI models for the HMC with its associated cutting dataset.

		Metric			
Force	Model	MAE (N)	RMSE (N)	MaxAE (N)	M-R (N)
F_X	ML	106.77 ± 85.97	120.53 ± 93.65	208.10 ± 128.00	204.9
	PI	52.84 ± 23.37	60.73 ± 26.45	122.17 ± 50.06	
F_Y	ML	102.70 ± 57.83	115.04 ± 62.44	208.36 ± 126.22	453.1
	PI	47.20 ± 34.60	55.68 ± 40.77	119.06 ± 80.65	
F_Z	ML	29.90 ± 24.74	34.92 ± 28.22	65.75 ± 44.40	77.17
	PI	16.01 ± 7.00	18.96 ± 8.17	39.02 ± 14.57	

In addition to the metric comparisons, visualizations of the modeled and measured forces are helpful to understand the success of each model. Fig. 3 shows the measured and modeled cutting forces as the feed per tooth increases for a series of six cutting passes at 2500 rpm on the VMC. The plots on the left-hand/right-hand side of the figure compare the PI-modeled/ML-modeled forces to the measured forces. In general, the PI model captures the force levels among the three cutting teeth. Accordingly, the model could be used in real time to detect a tooth breakage and the force levels among the teeth could be used to monitor runout of the end mill. In contrast, the ML model does not capture the variations of the force level for each tooth. Furthermore, as the general force level increases with the feed per tooth, the PI model captures this increase in force while the ML model fails to do so. Note that the measured forces in Fig. 3 for the PI and ML models are slightly different due to dissimilar model filtering operations on the force signals.

Similarly, Fig. 4 shows the measured and modeled cutting forces as the feed per tooth increases for a series of six cutting passes at 5000 rpm on the HMC. The plots on the left-hand/right-hand side of the figure compare the PI-modeled/ML-modeled forces to the measured forces. Compared to the cuts performed on the VMC, the cuts performed on the HMC do not exhibit as much variation among the forces for each of the three cutting teeth, perhaps because the end mill of the HMC is in a heat shrink holder. Nonetheless, the PI and ML models capture the nominal force levels and dominant frequencies among the three cutting teeth, except for two outliers produced by the ML model, as seen in Fig. 4h and Fig. 4l.

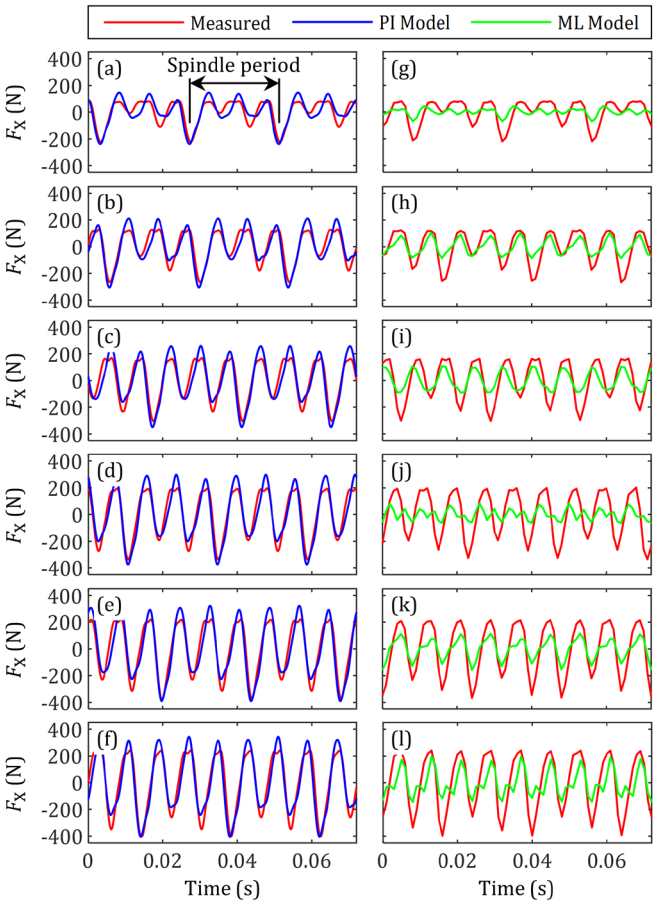

Fig. 3. Measured AC X-axis forces on the VMC for the three-fluted end mill spinning at 2500 rpm with the modeled forces for the (a-f) PI model and the (g-l) ML model with passes of increasing feed per tooth from 25.4 µm (0.001 in) to 152.4 µm (0.006 in).

Finally, Fig. 5 shows the modeled force range versus the measured force range for all cutting passes performed on the VMC (37 passes) and the HMC (18 passes). The plots on the left-hand/right-hand side of the figure compare the PI-modeled/ML-modeled force ranges to the measured force ranges. Being imperfect, the models produce estimated forces with ranges that are different from the measured force ranges. Hence, the plot markers do not typically coincide with the dashed identity lines. As seen in Fig. 5, the PI-modeled and ML-modeled force ranges may be significantly different from the measured ranges. However, the PI-modeled markers follow nominally linear trends as the feed per tooth increases, which is promising for process monitoring and optimization, while the trends of the ML-modeled force ranges are not nominally linear. This fact is understandable, since ML-based models typically lack a sufficient ability to extrapolate, which is needed because the cutting force magnitudes are more than 10X greater than those on which the models were trained. Nonetheless, Fig. 5 shows that the ML models do not produce enormously large outliers during extrapolation.

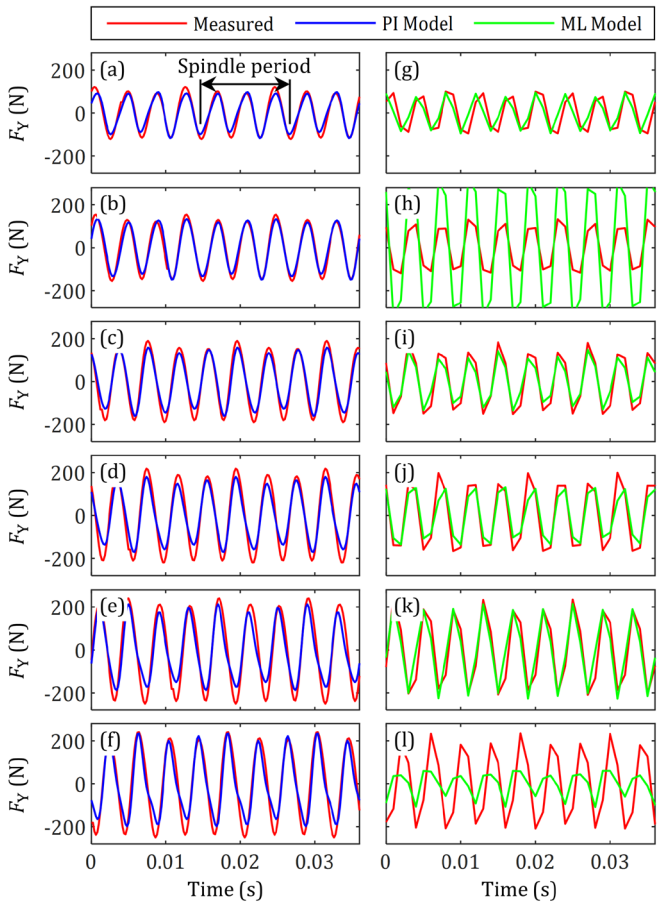

Fig. 4. Measured AC Y-axis forces on the HMC for the three-fluted end mill spinning at 5000 rpm with the modeled forces for the (a-f) PI model and the (g-l) ML model with passes of increasing feed per tooth from 25.4 µm (0.001 in) to 152.4 µm (0.006 in).

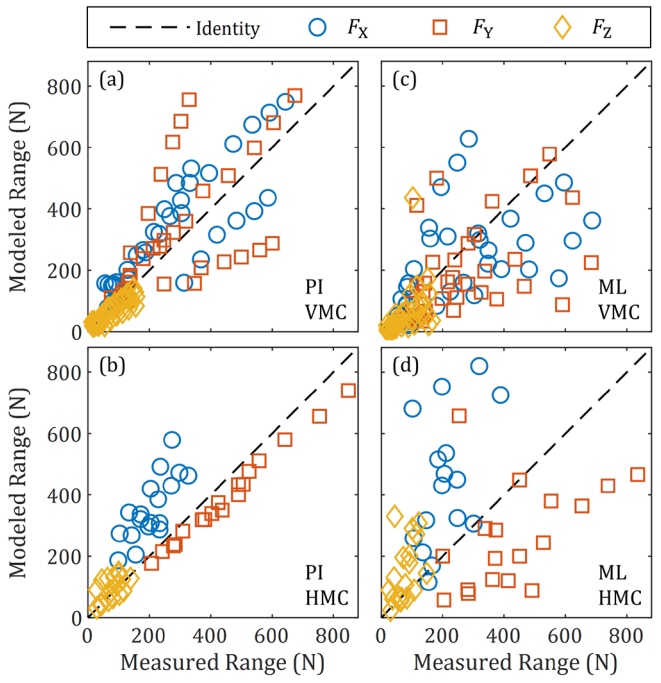

Fig. 5. Modeled force range versus the measured force range for all cutting passes, using the (a) PI model for the VMC, (b) PI model for the HMC, (c) ML model for the VMC, and (d) ML model for the HMC.

7. Conclusions

Two data-driven methods that estimate three-dimensional cutting forces from on-machine accelerometer measurements were compared with data measured during milling operations on two machine tools. One method uses machine learning (ML) while another uses a physics-inspired (PI) data-driven approach to estimate forces from accelerations. The PI models estimated the cutting forces with mean absolute errors of about 20 percent of the mean force ranges, which was generally better than the performance of the ML models. Nonetheless, both methods show the potential for monitoring real-time cutting forces via accelerometer measurements, to provide intelligence for the optimization of parts production.

Acknowledgements

The authors thank the Fabrication Technology Office at NIST and machining support personnel at the University of Tennessee, Knoxville and Oak Ridge National Laboratory for their significant contributions towards the experimental setup.

NIST disclaimer

Certain commercial equipment, instruments, or materials are identified in this paper in order to specify the experimental procedure adequately. Such identification is not intended to imply recommendation or endorsement by NIST, nor is it intended to imply that the materials or equipment identified are necessarily the best available for the purpose. This material is declared a work of the U.S. Government and is not subject to copyright protection in the United States. Approved for public release; distribution is unlimited.

References

[1] Teti R, Jemielniak K, O'Donnell G, Dornfeld D (2010) Advanced Monitoring of Machining Operations. *CIRP Annals - Manuf Technol* 59(2):717-739.
[2] Cao HR, Zhang XW, Chen XF (2017) The Concept and Progress of Intelligent Spindles: A Review. *Int J Mach Tools Manuf* 112:21-52.
[3] Postel M, Aslan D, Wegener K, Altintas Y (2019) Monitoring of Vibrations and Cutting Forces with Spindle Mounted Vibration Sensors. *CIRP Annals - Manuf Technol* 68(1):413-416.
[4] Wang C, Zhang X, Qiao B, Cao H, Chen X (2019) Dynamic Force Identification in Peripheral Milling Based on CGLS Using Filtered Acceleration Signals and Averaged Transfer Functions. *J Manuf Sci Eng* 141(6):064501.
[5] Ramsauer C, Leitner D, Habersohn C, Schmitz T, Yamazaki K, Bleicher F (2023) Flexure-Based Dynamometer for Vector-Valued Milling Force Measurement. *J Mach Eng* 23(1):47-56.
[6] Gomez M, Schmitz T (2022) Stability Evaluation for a Damped, Constrained-Motion Cutting Force Dynamometer. *J Manuf Mater Process* 6(1):23.
[7] Gomez M, Honeycutt A, Schmitz T (2021) Hybrid Manufactured Dynamometer for Cutting Force Measurement. *Manuf Lett* 29:65-69.
[8] Gomez M, Schmitz T (2020) Low-Cost, Constrained-Motion Dynamometer for Milling Force Measurement. *Manuf Lett* 25:34-39.
[9] Gomez M, Schmitz T (2019) Displacement-Based Dynamometer for Milling Force Measurement. *Procedia Manuf* 34:867-875.
[10] Vogl GW, Regli DA, Corson GM (2022) Real-Time Estimation of Cutting Forces Via Physics-Inspired Data-Driven Model. *CIRP Annals - Manuf Technol* 71(1):317-320.
[11] Fabro J, Vogl GW, Qu Y (2022) Run-Time Cutting Force Estimation Based on Learned Nonlinear Frequency Response Function. *J Manuf Sci Eng* 144(9)